Human Molecular Genetics, 2012, Vol. 21, No. 9 **1945–1953**
doi:10.1093/hmg/dds004
Advance Access published on January 6, 2012

BBS proteins interact genetically with the IFT pathway to influence SHH-related phenotypes

Qihong Zhang[1], Seongjin Seo[1], Kevin Bugge[1], Edwin M. Stone[2] and Val C. Sheffield[1,*]

[1]Department of Pediatrics and [2]Department of Ophthalmology and Visual Sciences, Howard Hughes Medical Institute, University of Iowa, 4181 MERF, Iowa City, IA 52242, USA

Received August 29, 2011; Revised November 18, 2011; Accepted January 4, 2012

There are numerous genes for which loss-of-function mutations do not produce apparent phenotypes even though statistically significant quantitative changes to biological pathways are observed. To evaluate the biological meaning of small effects is challenging. Bardet–Biedl syndrome (BBS) is a heterogeneous autosomal recessive disorder characterized by obesity, retinopathy, polydactyly, renal malformations, learning disabilities and hypogenitalism, as well as secondary phenotypes including diabetes and hypertension. BBS knockout mice recapitulate most human phenotypes including obesity, retinal degeneration and male infertility. However, BBS knockout mice do not develop polydacyly. Here we showed that the loss of BBS genes in mice result in accumulation of Smoothened and Patched 1 in cilia and have a decreased Shh response. Knockout of *Bbs7* combined with a hypomorphic *Ift88 allele (orpk* as a model for Shh dysfuction) results in embryonic lethality with e12.5 embryos having exencephaly, pericardial edema, cleft palate and abnormal limb development, phenotypes not observed in *Bbs7*$^{-/-}$ mice. Our results indicate that BBS genes modulate Shh pathway activity and interact genetically with the intraflagellar transport (IFT) pathway to play a role in mammalian development. This study illustrates an effective approach to appreciate the biological significance of a small effect.

INTRODUCTION

The use of loss-of-function mutations is an informative approach to identify the functions of a given gene. Some loss-of-function mutations generate dramatic phenotypes in model systems, and these mutations have been pivotal to understanding biological pathways and molecular mechanisms for human diseases. However, numerous genes do not produce apparent phenotypes when knocked out, even though statistically significant quantitative changes to biological pathways are observed. To evaluate the biological meaning of these small effects is a scientific challenge.

Cilia are microtubule-based structures that extend from the cell surface of most cells and are classified as either motile or primary cilia (immotile). The importance of cilia is highlighted by defects in cilia that lead to the development of a wide range of human diseases termed ciliopathies, which include primary ciliary dyskinesis, polycystic kidney disease, nephronophthisis, Joubert syndome, Senior–Loken syndrome, Meckel–Gruber syndrome, oro-facial-digital syndrome, Alstrom syndrome and Bardet–Biedl syndrome (BBS).

BBS (OMIM 209900) is an autosomal recessive genetic disorder characterized by obesity, retinopathy, polydactyly, renal malformations, learning disabilities and hypogenitalism, as well as diabetes and hypertension. To date, 16 BBS genes have been shown to independently cause the disorder (1–13). Seven BBS proteins (BBS1, BBS2, BBS4, BBS5, BBS7, BBS8 and BBS9) along with an interacting protein known as BBIP10 form a complex called the BBSome, which is involved in ciliary membrane biogenesis (14). Although several ciliary membrane proteins have been shown to require the BBSome for transport to cilia (15,16), the physiological relevance of some of these ciliary membrane proteins to BBS phenotypes are currently unknown.

BBS knockout mice display most human BBS phenotypes including obesity, retinal degeneration and male infertility. However, unlike human BBS patients, BBS knockout mice do not develop polydactyly (17–20). Most polydactyly phenotypes typically have the sonic hedgehog (Shh) pathway defects and the Shh pathway is known to control tissue patterning during mammalian development. Shh activates the pathway by binding to its receptor Patched 1 (Ptch1) releasing

*To whom correspondence should be addressed. Tel: +1 3193356937; Fax: +1 3193357588; Email: val-sheffield@uiowa.edu

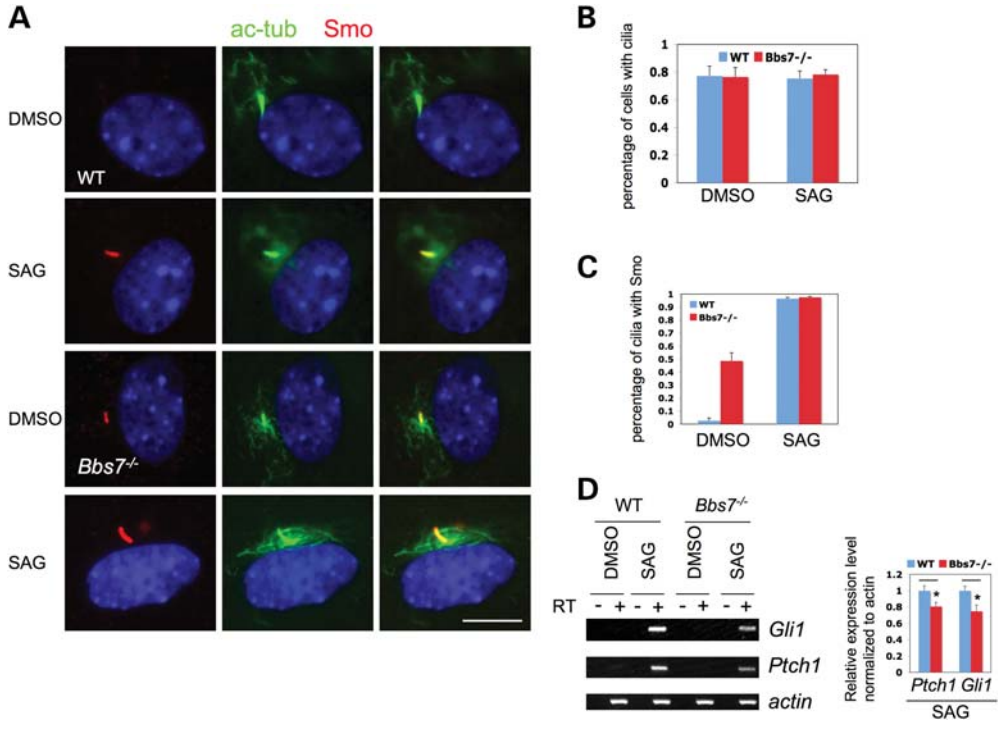

Figure 1. The BBSome regulates Smo ciliary localization and Shh signaling. (**A**) Cultured MEF cells from WT and *Bbs7*$^{-/-}$ mice stimulated with dimethyl sulfoxide (DMSO) or with Shh pathway activator N-Methyl-N′-(3-pyridinylbenzyl)-N′-(3-chlorobenzo[b]thiophene-2-carbonyl)-1,4-diaminocyclohexane (SAG) were stained with anti-acetylated tubulin (green) as a cilia marker and anti-Smo (red). (**B**) Quantitation of percentage of cells with cilia with or without SAG treatment found no differences between WT and *Bbs7*$^{-/-}$ MEF cells. (**C**) Quantitation of percentage of cilia with Smo staining when treated with DMSO or SAG. (**D**) qPCR for *Gli1* and *Patched 1* from cultured *Bbs7*$^{-/-}$ MEF cells stimulated with SAG showed a 20–30% decreased Shh pathway output compared with WT MEF cells when normalized to actin. Scale bar represents 10 μm. $^{*}P < 0.02$.

Smoothened (Smo) from inhibition. Activated Smo transduces the signal via Gli transcription factors. There are three Gli proteins (Gli1, Gli2 and Gli3) in vertebrates. Gli2 and Gi3 are the primary regulators of the pathway during development (21).

It is well established that cilia are required for hedgehog pathway signaling (22–27). BBS mutant mice have motile cilia defects in brain ependymal cells, trachea epithelial cells and sperm flagella, but they do not have apparent primary cilia morphological defects, although the primary cilium may have functional deficits (17–20). While the loss of BBS function has been shown to result in wingless-type MMTV integration site (Wnt)/planar cell polarity defects (28–31), it is not clear whether the loss of BBS genes also affect the Shh pathway. The lack of the polydactyly phenotype in BBS mutant mice prompted us to investigate the underlying molecular defects in BBS mutant mice. Here we showed that Smo and Ptch1 are endogenous cargos of the BBSome and that the loss of BBS genes in mice results in accumulation of Smo and Ptch1 in cilia and lead to a quantitative decrease in Shh response. To evaluate the biological significance of this quantitative decrease in Shh signaling, we investigated whether knockout of BBS function could modify another cilia-related mutation, a hypomorphic allele of Ift88 known as *orpk* (oak ridge polycystic kidney). We show that homozygous knockout of *Bbs7* combined with the homozygous *Ift88 orpk* allele results in embryonic lethality. The e12.5 embryos have exencephaly, pericardial edema, cleft palate and polydactyly. Our results indicate that BBS genes modulate Shh pathway activity and interact genetically with the intraflagellar transport (IFT) pathway to influence mammalian development.

RESULTS

The BBSome regulates Smo ciliary localization and Shh signaling

One of the cardinal features of BBS is post-axial polydactyly, which is present in most human BBS patients. However, none of the BBS mutant mice (*Bbs1*$^{M390R/M390R}$ knockin, *Bbs2*$^{-/-}$, *Bbs4*$^{-/-}$, *Bbs6*$^{-/-}$ and *Bbs7*$^{-/-}$) develop polydactyly (17–20). Most mutant mice that have polydactyly have defective Shh signaling; therefore, we examined the Shh pathway in BBS mutant mice. We isolated mouse embryonic fibroblast (MEF) cells and embryonic brain cells from wild-type (WT) and Bbs mutant mice (*Bbs1*$^{M390R/M390R}$ knockin, *Bbs2*$^{-/-}$, *Bbs4*$^{-/-}$ and *Bbs7*$^{-/-}$). MEF and embryonic brain cells are known to respond to hedgehog ligand stimulation (32). Smo, one of the hedgehog pathway components, localizes to cilia when stimulated by Shh ligand or by pathway agonists such as N-Methyl-N′-(3-pyridinylbenzyl)-N′-(3-chlorobenzo[b]thiophene-2-carbonyl)-1,4-diaminocyclohexane (SAG). To determine whether the loss of the BBSome affects Smo ciliary localization, we stimulated cultured WT and *Bbs7*$^{-/-}$ MEF cells with the Shh pathway agonist SAG. About 45% of cilia are Smo positive in BBS mutant MEF cells even without stimulation with SAG (Fig. 1A and C) compared

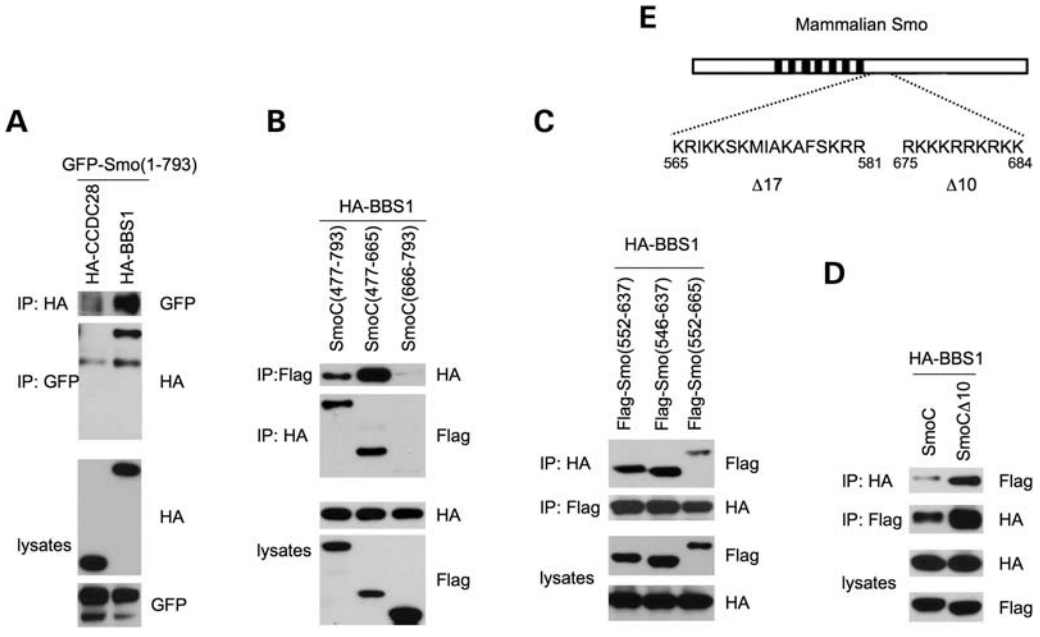

Figure 2. The BBSome interacts with the C-terminus of Smo. Shown are reciprocal immunoprecipitation assays in 293T cells of hemagglutinin (HA)-tagged BBS1 with GFP-tagged Smo (**A**) and HA-tagged Ccdc28 as a negative control (**B**). HA-BBS1 interacts with the Flag-tagged Smo C-terminal tail, which contains two stretches of basic amino acids. BBS1 interacts with the Smo C-terminal region that contains a stretch of 17 amino acids rich in basic residues, but not with an Smo C-terminal region that contain a stretch of only 10 basic amino acids. (**C**) Domain-binding analysis reveals that BBS1 binds to the Smo C-terminal region between amino acid 552–637. (**D** and **E**) A stretch of 10 basic amino acids in the Smo C-terminal tail regulates the interaction between Smo and BBS1.

with <5% of WT MEF cells having Smo staining. SAG stimulation increases the percentage of cilia that are Smo positive to nearly 100% in both WT and *Bbs7*$^{-/-}$ cells (Fig. 1A and C). Similar results were obtained with cultured brain cells (data not shown). These data indicate that the loss of BBS increases the basal level of Smo in cilia, perhaps by affecting Smo retrograde transport out of cilia, since BBS genes have been shown to be required for retrograde transport in model systems including zebrafish and *Chlamydomonas reinhardtii* (33,34). Similar results are obtained using MEF cells from *Bbs1*$^{M390R/M390R}$ knockin, *Bbs2*$^{-/-}$ and *Bbs4*$^{-/-}$ (data not shown). To determine whether the increased ciliary localization of Smo activates the Shh pathway, we examined the expression of *Gli1* and *Ptch1*, two genes whose expressions are upregulated when the Shh pathway is activated. To our surprise, the increased ciliary localization of Smo in the absence of normal BBS genes results in a 20–30% decrease in Shh pathway activation in MEF cells (Fig. 1D). These results are consistent with the notion that ciliary localized Smo has two states: inactive and active. Ciliary localization of Smo is not sufficient to activate the pathway (25). The BBSome may modulate the conversion of Smo from the inactive to the active state within cilia.

The BBSome interacts with Smo

To further analyze how the loss of the BBSome affects ciliary localization of Smo, we examined whether the BBSome interacts physically with Smo. This was performed by co-transfection of each individually hemagglutinin (HA)-tagged BBSome component (BBS1, 2, 4, 5, 7, 8 and 9) with either GFP- or Flag-tagged Smo. Using a reciprocal immunoprecipitation assay, we demonstrated that full-length Smo interacts with several BBSome subunits with BBS1 showing the strongest interaction (Fig. 2A and Supplementary Material, Fig. S1D). BBS1 specifically binds to the C-terminal cytoplasmic tail of Smo (amino acids 477–793) (Fig. 2B). It has been previously demonstrated that the minimal region of Smo that is required for activity comprises amino acids 1–637 (35). We demonstrated with deletion analysis that BBS1 binds to the C-terminal cytoplasmic tail of Smo between amino acids 552–637 (Fig. 2C), overlapping the critical domain for Smo activity. Constitutively active or inactive mutations of Smo do not affect ciliary localization of Smo, nor do they affect interaction with BBS1 (Supplementary Material, Fig. S1).

Studies from *Drosophila* show that hedgehog induces phosphorylation of multiple Ser/Thr residues to antagonize multiple Arg clusters in the Smo C-terminal cytoplasmic tail to induce an Smo conformation change and activate the pathway (36). Vertebrate Smo also contains two clusters of basic amino acids in the cytoplasmic tail (Fig. 2E), and Shh induces a conformational change (36). We asked whether this conformational switch regulates the interaction with the BBSome. Deletion of a stretch of 10 basic amino acids in the Smo C-terminal tail enhanced its interaction with BBS1 (Fig. 2D), whereas deleting a stretch of 17 basic amino acids has minimal effect on the interaction with BBS1. None of these deletion mutations affects the ciliary localization of Smo (Supplementary Material, Fig. S1).

The BBSome regulates Ptch1 ciliary localization

Ptch1, another membrane protein of the hedgehog pathway, is a hedgehog receptor and localizes to the cilia. To determine

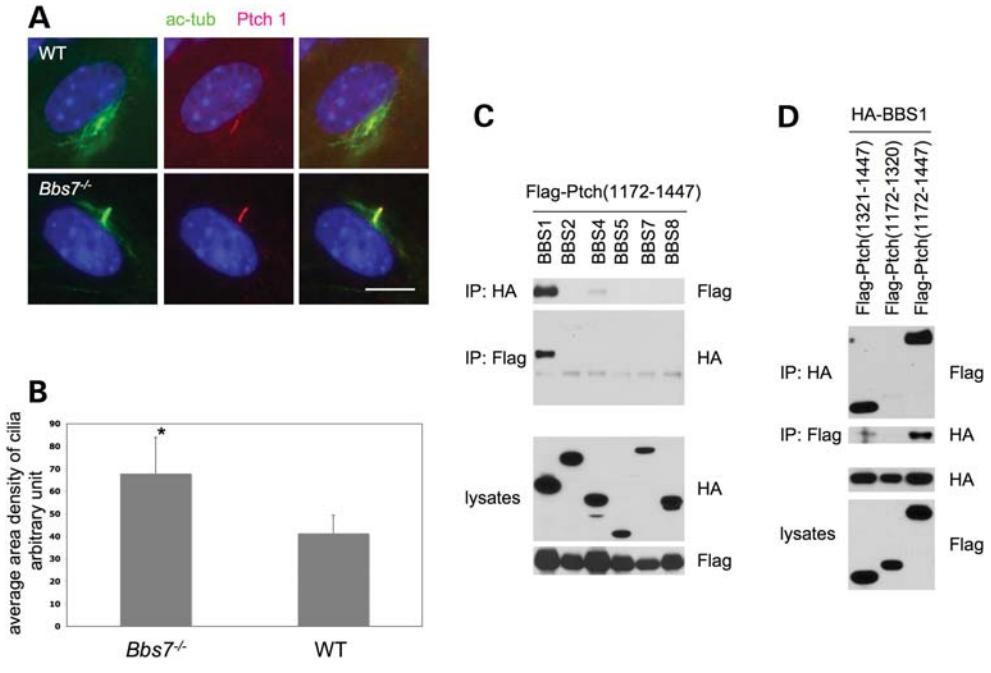

Figure 3. The BBSome regulates Ptch1 ciliary localization. (**A**) Cultured MEF cells from WT and *Bbs7*$^{-/-}$ mice stimulated with the Shh pathway activator, SAG, were stained with anti-acetylated tubulin (green) as a cilia marker and anti-Ptch1 (red). (**B**) Quantitation of the intensity of Ptch1 staining inside cilia when treated with SAG. *Bbs7*$^{-/-}$ MEF cells have statistically higher amount of Ptch1 inside the cilia compared with WT MEF cells. (**C**) Shown are reciprocal immunoprecipitation assays in 293T cells of HA-tagged each BBSome components with Flag-tagged Ptch1. Ptch1 interacts with the BBSome through the BBS1 subunit. (**D**) BBS1 interacts with the C-terminal tail of Ptch1 between amino acid 1322–1447. Scale bar represents 10 μm.

whether the BBSome also regulates Ptch1 ciliary localization, we stained MEF cells from WT and *Bbs7*$^{-/-}$ mice with antibody against Ptch1. Increased Ptch1 staining was detected in the cilia of *Bbs7*$^{-/-}$ MEF cells compared with WT MEF cells when stimulated with SAG (Fig. 3A and B). Similar results are obtained using MEF cells from *Bbs1*$^{M390R/M390R}$ knockin, *Bbs2*$^{-/-}$ and *Bbs4*$^{-/-}$ (data not shown). This result may explain the deceased Shh response in BBS knockout cells as Ptch1 is a negative regulator of the Shh pathway.

To further analyze how the loss of BBSome affects Ptch1 ciliary localization, we tested whether the BBSome directly interacts with Ptch1. Co-transfection of Flag-tagged C-terminal cytoplasmic tail of Ptch1 along with HA-tagged individual BBSome subunits (BBS1, 2, 4, 5, 7, 8 and 9) revealed that the C-terminal tail of Ptch1 interacts strongly with BBS1 (Fig. 3C), while no interaction or very weak interaction was detected with other BBSome subunits. Structure analysis using SMART does not reveal any domains analogous to any known proteins in the C-terminal tail of Ptch1 and only four low-complexity regions are found. We therefore chose to make deletions that separate these four low-complexity regions and showed that amino acids 1322–1447 of the C-terminus of Ptch1 are required for binding to BBS1 (Fig. 3D).

Genetic interaction between *Bbs7* and *Ift88* affects mammalian development

Although BBS knockout mice do not develop polydactyly, our *in vitro* studies indicate statistically significant differences in the Shh pathway activation in response to Shh agonist, suggesting that the loss of BBS proteins may sensitize mice to hedgehog pathway defects. We reasoned that further reduction in the Shh response in BBS mutant mice would result in polydactyly. *Ift88* hypomorphic ORPK mice have greatly decreased Ift88 protein levels, improper IFT complex B formation, hedgehog signaling defects and polydactyly (Supplementary Material, Fig. S5). Interestingly, ORPK MEF cells also accumulate Smo in the cilium even without SAG stimulation (Supplementary Material, Fig. S5C), consistent with the finding that polycystin-2 is accumulated inside the cilium in ORPK mice (37). The BBSome interacts with IFT proteins when expressed in cells and co-localizes at punctae inside the cilium (Supplementary Material, Fig. S6), although the endogenous protein interaction cannot be detected (Supplementary Material, Fig. S5B). In ORPK mice, polydactyly is only displayed in the hindlimb (38). Although ORPK mice have multiple organ defects including cystic kidneys, hydrocephalus, liver fibrosis, pancreatitis and retinal degeneration (39–41), they survive to adulthood on a C57BL/6 background and otherwise appear to be normal. It has been shown that knocking down any BBSome subunit in cell culture resulted in the loss of BBSome formation (42). We have confirmed that there is no BBSome formation in the absence of Bbs7 (data not shown). Therefore, we use *Bbs7*$^{-/-}$ as a surrogate for the loss of the BBSome. When we crossed *Bbs7*+/−; *orpk*+/− double heterozygotes with each other. No double mutant offspring were found at weaning out of 145 offspring, suggesting that they may die prenatally or perinatally. We therefore closely followed the mice at birth and genotyped 99 P0 offspring. No double mutants were found, indicating prenatal death. Timed matings were set up and fetuses were collected at e11.5–13.5. Five of 74 (6.7%) fetuses were

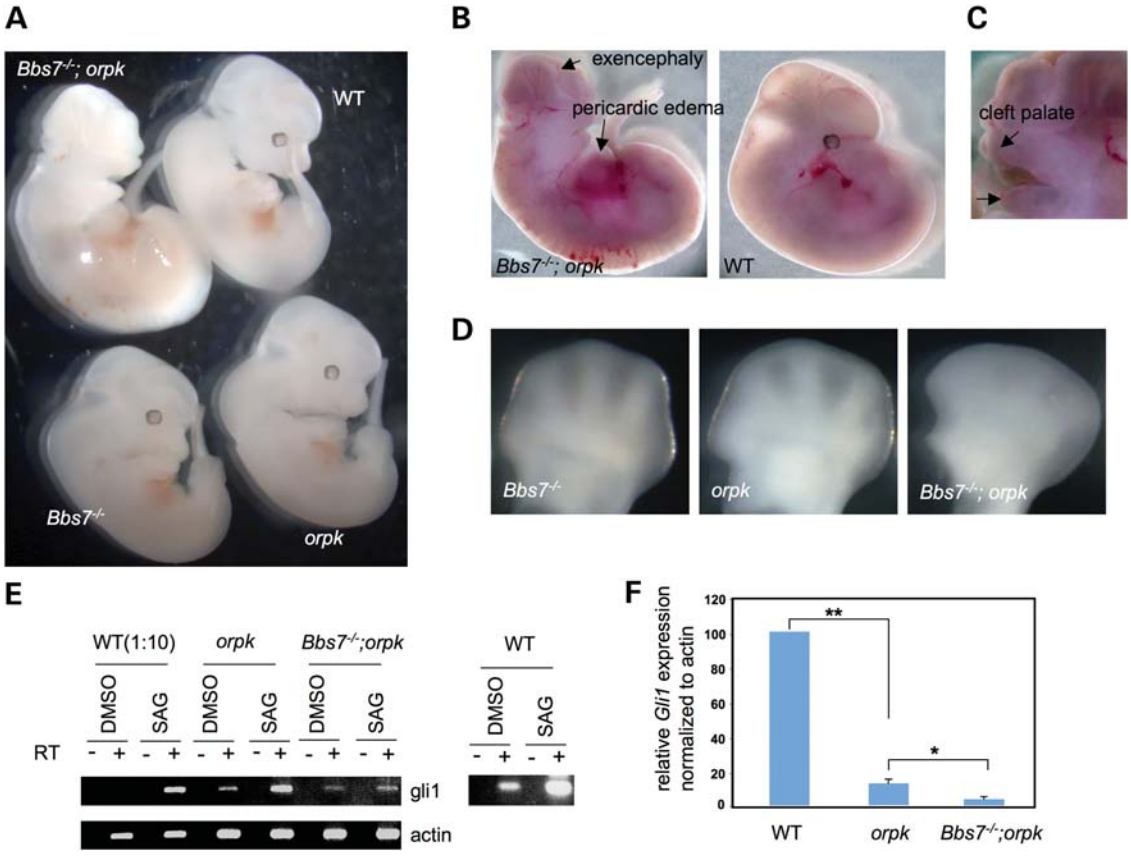

Figure 4. Genetic interaction between *Bbs7* and *Ift88* regulates mammalian development. *Bbs7* and *Ift88orpk* double mutant at e12.5 showed gross morphological defects (**A**), exencephaly, pericardial edema and lack of eyes (**B**), cleft palate (**C**) and limb developmental delay and polydactyly (**D**). MEF cells from *Bbs7* and *Ift88orpk* double mutant have further decreased the Shh response by RT–PCR assay of *Gli1* expression level compared with *Ift88orpk* single mutant when treated with SAG (**E**), we diluted WT cDNA by 10-fold in order to see *Gli1* band in double mutant.

double mutants (6.25% predicted based on Mendelian ratios at two independent loci). Double-mutant embryos have exencephaly, pericardial edema, no eye development and cleft palate (Fig. 4). Neither the homozygous single mutants, nor homozygous single mutant animals that were heterozygous at the other locus had phenotypes similar to the double homozygous mutant mice. Limb development of the double mutant embryos is delayed in that e11.5 limbs morphologically look like e10.5 WT limbs and e12.5 limbs morphologically look like e11.5 WT limbs and lack calcification. In addition to the delayed morphological appearance, the e12.5 limb buds of the double-mutant embryos are broad compared with e11.5 WT limb buds, suggesting polydactyly (Fig. 4D). Double mutants do not survive beyond e12.5, which precluded us from identifying the exact digit numbers. These findings indicate that double mutants have severe Shh pathway defects and resemble complete knockout of IFT genes. Indeed, MEF cells from double mutants have further decreased Shh response when treated with SAG compared with *Ift88(orpk)* single mutant cells as demonstrated by quantitative polymerase chain reaction (PCR) of *Gli1*, a direct target of Shh pathway activation (Fig. 4E and F). The neural tubes, other than the brain region, are closed and no apparent Wnt/PCP (planar cell polarity) defects are found in the double-mutant embryos. Together, these results indicate that BBS and IFT genes interact genetically during mammalian development.

DISCUSSION

The importance of cilia is highlighted by the fact that numerous diseases have been associated with defects in cilia structure or cilia function. It is well established that cilia are required for the hedgehog pathway (23–26,43,44). Involvement of cilia in Wnt/β-catenin and Wnt/PCP signaling pathways are more controversial (45–47), although accumulating evidence supports that cilia are also important for these pathways (30,48–51). It has been reported that BBS knockout mice develop phenotypes similar to Wnt/PCP pathway mutants including midbrain exencephaly and open eyelids (30). However, we have not detected such defects in any of the BBS mutant mice ($Bbs1^{M390R/M390R}$ knockin, $Bbs2^{-/-}$, $Bbs4^{-/-}$, $Bbs6^{-/-}$ and $Bbs7^{-/-}$) either on 129Sv, C57BL6 or mixed genetic backgrounds (our unpublished data). We also recover mendelian ratios of embryos at e12.5. One possible explanation for the discrepancy between our mice and other reported mouse models is that BBS mutant mice generated in our laboratory were generated using homologous recombination, while BBS mutant mice that showed PCP defects were generated by gene-trapping methodology.

The accumulation of endogenous Smo in cilia implies that transport of Smo out of cilia is dependent on BBSome function. This result is reminiscent of the localization of Smo in *Dync2h1* mutant MEFs (46,52). In *Dync2h1* mutant MEFs,

Smo is constitutively present in cilia but the presence of Smo is not sufficient to activate the hedgehog pathway. While stimulation of *Dync2h1* MEF cells with SAG does not increase Smo ciliary localization, stimulation of BBS mutant MEF cells with SAG further increases Smo ciliary localization, indicating that BBS mutant MEF cells can respond to Shh pathway activation, although the response is diminished. This difference could explain why *Dync2h1* mutant mice have developmental defects including polydactyly, while BBS mutant mice do not. Consistent with the results from mouse studies, skin fibroblast cells derived from the most common human BBS mutation: BBS1M390R also accumulate Smo in the cilia even without SAG stimulation (Supplementary Material, Fig. S8), indicating that the underlying mechanism is conserved between mouse and humans.

The accumulation of both Smo and Ptch1 in BBS null MEF cells is consistent with genetic studies in zebrafish in which knockdown of BBS gene expression results in the delay of melanosome retrograde transport (34), which is mediated by the dynein complex. In an attempt to identify potential binding partners for BBS proteins, we performed yeast 2-hybrid screens using BBS proteins as baits. Interestingly, cytoplasmic dynein light intermediate chain 1 and $p150^{Glued}$ dynactin interact with BBS proteins. These interactions were confirmed *in vivo* using co-immunoprecipitation assays (Supplementary Material, Fig. S3). Considering that the BBSome has been suggested as a cargo for the IFT complex, and reportedly serves as a bridge between IFT complex A and IFT complex B in *C. elegans* (33,53), it was somewhat surprising to us that no IFT proteins were identified in our Y2H screen. One explanation is that the interaction requires the intact BBSome and the intact IFT complex, not individual components. The cargo—BBSome—dynein complex link could be an underlying molecular mechanism involved in BBS phenotypes. How the loss of BBS affects the cargo–dynein complex interaction will be the focus of future work.

Several possibilities can explain why increased ciliary localization of Smo did not result in increased Shh pathway activation. First, Smo localized within cilia has two states: inactivated and activated (25). The BBSome may be required to modulate the conversion from the inactive to the active state inside the cilium. Secondly, Ptch1, a negative regulator of the hedgehog pathway, normally moves out of cilia when the pathway is activated. However, accumulation of Ptch1 within cilia in the absence of BBS components may inhibit Shh pathway activation. Recent studies have shown that Shh ligand transmits the signal through regulating Gli-Su(fu) ciliary entry and subsequent dissociation of Gli and Su(fu) leading to the activation of Gli transcription factors and activation of the pathway (54–56). Although the BBSome can interact with Gli1, Gli2 and Su(fu) (Supplementary Material, Fig. S4), unlike *Dync2h1* MEF cells, BBS mutant MEF cells do not accumulate Gli2 inside cilia (Supplementary Material, Fig. S7), suggesting that the BBSome may transport specific ciliary membrane proteins.

In *Drosophila*, the atypical kinesin Costal-2 serves as an adaptor between transmembrane transducer Smo and the transcriptional effector Cubitus interruptus (57). The mammalian homolog of Costal-2 is kif7. Whether kif7 has a similar role as Costal-2 to bridge Smo to Gli proteins is currently unknown. Physical interactions between the BBSome, Smo C-terminus and Gli-Su(fu) suggests that the BBSome may play a role in this process. Attempts to detect the physical interactions among the endogenous BBSome, Smo and Gli-Su(fu) were unsuccessful. This is not surprising, considering that the BBSome is a part of a transport system, and we thus expect that the interactions between the BBSome and its cargoes [Smo, Ptch1 and Gli-Su(fu) or other hedgehog pathway components] will be transient and weak due to the need to constantly load and release cargoes. One illustrative example is that IFT complexes are known to require both the antegrade motor, kinesin II and the retrograde motor, dynein, to power the movement of IFT particles. No endogenous interactions between IFT complexes and motors have been detected. Another example is that the BBSome and IFT complexes co-localize inside *Chlamydomonoas flagella* and the BBSome appears to be transported by IFT particles (33), yet the purified BBSome does not contain IFT components. Another factor that may limit our detection of endogenous protein interactions is that the BBSome may only interact with hedgehog pathway components inside cilia, and only a portion of these proteins (both the BBSome and hedgehog pathway components) actually localize to cilia. Elevation of protein concentrations inside cells by overexpressing them will increase the chance to detect this type of interaction. That Smo co-localizes with BBSome particles inside the cilium (Supplementary Material, Fig. S2) indicates that they may interact *in vivo*.

The phenotypes of *Bbs7* and *Ift88orpk* double mutants resemble those of complete knockout of IFT genes, indicating that they lose responsiveness to Shh ligand. Even though single homozygous mutants of either gene have diminished Shh responsiveness, single mutant mice survive to adulthood, in stark contrast to the double mutants. Creation of double mutants is an effective approach to evaluate the biological meaning of small effects like we observe for Shh pathway activation when BBS genes are deleted. The delayed development of the limb in the double-mutant embryos, together with the fact that the double mutants do not survive beyond e12.5, precludes the determination of the exact nature of digit development in the double mutants. To further support that double mutants might develop polydactyly, MEF cells from double mutants fail to form cilia (manuscript in preparation), unlike in any single mutants. Future deletion of BBS genes in the limb using Prx1-cre, which is expressed in the limb mesenchymal cells, along with crosses to *Ift88orpk* mice, will provide a definitive answer to this question.

MATERIALS AND METHODS

Antibodies and reagents

The hypomorphic *Ift88* mouse, Oak Ridge Polycystic Kidney (orpk mouse), was kindly provided by Dr Gregory Pazour (University of Massachusetts Medical School, Worcester). SAG was purchased from Calbiochem (Gibbstown, NJ, USA). Rabbit anti-Smo antibody was from Abcam (Cambridge, MA, USA), anti-acetylated tubulin was purchased from Sigma (St. Louis, MO, USA), rabbit anti-Su(fu) and goat anti-IFT57 antibodies were purchased from Santa Cruz

Biotechnology (Santa Cruz, CA, USA). Rabbit anti-IFT57, IFT88, IFT20 and IFT81 were purchased from Proteintech (Chicago, IL, USA). Anti-Gli2 antibody is a gift from Dr Jonathan T. Eggenschwiler (Princeton University, Princeton, NJ, USA), anti-Patched 1 antibody is a gift from Dr Rajat Rohatgi (Stanford University, Stanford, CA, USA). Alexa 488-conjugated and Alexa 568-conjugated secondary antibodies were purchased from Invitrogen (Carlsbad, CA, USA).

Generation of MEF cells

WT and mutant (*Bbs7*$^{-/-}$, *Bbs2*$^{-/-}$, *Bbs4*$^{-/-}$ and *Bbs1*$^{M390R/M390R}$ knockin) primary MEFs were generated from embryonic day 12.5 embryos and cultured in Dulbecco's modified Eagle medium with 10% fetal bovine serum and penicillin/streptomycin. To induce cilia formation, MEF cells were grown to 80–90% confluency and serum starved for 24 h; cells were treated with dimethyl sulfoxide (DMSO) or 100 nM SAG for 16–20 h.

Immunoprecipitation

Differentially tagged human BBS genes (BBS1, BBS2, BBS4, BBS5, BBS7, BBS8 and BBS9) were co-transfected into 293T cells. Forty-eight hours after transfection, the cells were lysed in lysis buffer (1× phosphate buffered saline (PBS), 1% Triton X-100 and protease inhibitor—Roche, Indianapolis, IN, USA) and spun at 14 000 rpm for 15 min at 4°C. The supernatants were cleared by incubation with protein G beads (Pierce, Rockford, IL, USA). Cleared lysates were incubated with antibodies against corresponding tags for 4 h. Protein G beads were then added and incubated for another 4 h. The beads were washed four times with lysis buffer and the interactions were detected by western blotting.

Immunofluorescence microscopy

Cells were fixed in 4% paraformaldyhyde in PBS and permeabilized with 0.2% Triton X-100 in room temperature for 7 min. Cells were washed 3× PBS and blocked with blocking buffer (1% bovine serum albumin in PBS). Primary antibodies were diluted in blocking buffer and incubated at room temperature for 1 h. Cells were washed 3× PBS, blocked with blocking buffer, then incubated with Alexa 488- or Alexa 568-labeled secondary antibodies (Invitrogen) for 45 min at room temperature. Nuclei were stained with DAPI (Sigma). The intensity of staining inside the cilia was measured using ImageJ.

Quantitative RT–PCR

RNA was isolated from DMSO- or SAG-treated MEF cells using TRIzol reagent (Invitrogen). cDNA was prepared from 1 μg of total RNA using SuperScript III reverse transcriptase (Invitrogen). Quantitative PCR was performed with SYBR Green Supermix (Bio-Rad) and Mx3000P qPCR System (Stratagene) with primers against mouse *Gli1* and *Patched 1*. Mouse actin was used as an internal control. Primer sequences are available upon request.

SUPPLEMENTARY MATERIAL

Supplementary Material is available at *HMG* online.

ACKNOWLEDGEMENTS

The authors thank Dr Gregory Pazour (University of Massachusetts Medical School, Worcester) for providing *Ift88orpk* mice, Dr Jonathan T. Eggenschwiler (Princeton University, Princeton) for anti-Gli2 antibody, Dr Rajat Rohatgi (Stanford University, Stanford) for anti-Patched 1 antibody. Dr Pao-Tien Chuang (University of California, San Francisco) for Flag-tagged Gli2 and Gli3 vectors.

Conflict of Interest statement. V.C.S. and E.M.S. are investigators of the Howard Hughes Medical Institute.

FUNDING

This work was supported by National Institute of Health grants [R01EY110298 and R01EY017168 (to V.C.S. and E.M.S.)]. Funding to pay the Open Access publication charges for this article was provided by Howard Hughes Medical Institute.

REFERENCES

1. Badano, J.L., Ansley, S.J., Leitch, C.C., Lewis, R.A., Lupski, J.R. and Katsanis, N. (2003) Identification of a novel Bardet–Biedl syndrome protein, BBS7, that shares structural features with BBS1 and BBS2. *Am. J. Hum. Genet.*, **72**, 650–658.
2. Chiang, A.P., Beck, J.S., Yen, H.J., Tayeh, M.K., Scheetz, T.E., Swiderski, R.E., Nishimura, D.Y., Braun, T.A., Kim, K.Y., Huang, J. *et al.* (2006) Homozygosity mapping with SNP arrays identifies TRIM32, an E3 ubiquitin ligase, as a Bardet-Biedl syndrome gene (BBS11). *Proc. Natl Acad. Sci. USA*, **103**, 6287–6292.
3. Chiang, A.P., Nishimura, D., Searby, C., Elbedour, K., Carmi, R., Ferguson, A.L., Secrist, J., Braun, T., Casavant, T., Stone, E.M. *et al.* (2004) Comparative genomic analysis identifies an ADP-ribosylation factor-like gene as the cause of Bardet–Biedl syndrome (BBS3). *Am. J. Hum. Genet.*, **75**, 475–484.
4. Fan, Y., Esmail, M.A., Ansley, S.J., Blacque, O.E., Boroevich, K., Ross, A.J., Moore, S.J., Badano, J.L., May-Simera, H., Compton, D.S. *et al.* (2004) Mutations in a member of the Ras superfamily of small GTP-binding proteins causes Bardet–Biedl syndrome. *Nat. Genet.*, **36**, 989–993.
5. Leitch, C.C., Zaghloul, N.A., Davis, E.E., Stoetzel, C., Diaz-Font, A., Rix, S., Alfadhel, M., Lewis, R.A., Eyaid, W., Banin, E. *et al.* (2008) Hypomorphic mutations in syndromic encephalocele genes are associated with Bardet–Biedl syndrome. *Nat. Genet.*, **40**, 443–448.
6. Li, J.B., Gerdes, J.M., Haycraft, C.J., Fan, Y., Teslovich, T.M., May-Simera, H., Li, H., Blacque, O.E., Li, L., Leitch, C.C. *et al.* (2004) Comparative genomics identifies a flagellar and basal body proteome that includes the BBS5 human disease gene. *Cell*, **117**, 541–552.
7. Mykytyn, K., Braun, T., Carmi, R., Haider, N.B., Searby, C.C., Shastri, M., Beck, G., Wright, A.F., Iannaccone, A., Elbedour, K. *et al.* (2001) Identification of the gene that, when mutated, causes the human obesity syndrome BBS4. *Nat. Genet.*, **28**, 188–191.
8. Mykytyn, K., Nishimura, D.Y., Searby, C.C., Shastri, M., Yen, H.J., Beck, J.S., Braun, T., Streb, L.M., Cornier, A.S., Cox, G.F. *et al.* (2002) Identification of the gene (BBS1) most commonly involved in Bardet–Biedl syndrome, a complex human obesity syndrome. *Nat. Genet.*, **31**, 435–438.
9. Nishimura, D.Y., Searby, C.C., Carmi, R., Elbedour, K., Van Maldergem, L., Fulton, A.B., Lam, B.L., Powell, B.R., Swiderski, R.E., Bugge, K.E. *et al.* (2001) Positional cloning of a novel gene on chromosome 16q causing Bardet–Biedl syndrome (BBS2). *Hum. Mol. Genet.*, **10**, 865–874.

10. Nishimura, D.Y., Swiderski, R.E., Searby, C.C., Berg, E.M., Ferguson, A.L., Hennekam, R., Merin, S., Weleber, R.G., Biesecker, L.G., Stone, E.M. *et al.* (2005) Comparative genomics and gene expression analysis identifies BBS9, a new Bardet–Biedl syndrome gene. *Am. J. Hum. Genet.*, **77**, 1021–1033.
11. Stoetzel, C., Laurier, V., Davis, E.E., Muller, J., Rix, S., Badano, J.L., Leitch, C.C., Salem, N., Chouery, E., Corbani, S. *et al.* (2006) BBS10 encodes a vertebrate-specific chaperonin-like protein and is a major BBS locus. *Nat. Genet.*, **38**, 521–524.
12. Stoetzel, C., Muller, J., Laurier, V., Davis, E.E., Zaghloul, N.A., Vicaire, S., Jacquelin, C., Plewniak, F., Leitch, C.C., Sarda, P. *et al.* (2007) Identification of a novel BBS gene (BBS12) highlights the major role of a vertebrate-specific branch of chaperonin-related proteins in Bardet–Biedl syndrome. *Am. J. Hum. Genet.*, **80**, 1–11.
13. Kim, S.K., Shindo, A., Park, T.J., Oh, E.C., Ghosh, S., Gray, R.S., Lewis, R.A., Johnson, C.A., Attie-Bittach, T., Katsanis, N. *et al.* (2010) Planar cell polarity acts through septins to control collective cell movement and ciliogenesis. *Science*, **329**, 1337–1340.
14. Nachury, M.V., Loktev, A.V., Zhang, Q., Westlake, C.J., Peranen, J., Merdes, A., Slusarski, D.C., Scheller, R.H., Bazan, J.F., Sheffield, V.C. *et al.* (2007) A core complex of BBS proteins cooperates with the GTPase Rab8 to promote ciliary membrane biogenesis. *Cell*, **129**, 1201–1213.
15. Berbari, N.F., Johnson, A.D., Lewis, J.S., Askwith, C.C. and Mykytyn, K. (2008) Identification of ciliary localization sequences within the third intracellular loop of G protein-coupled receptors. *Mol. Biol. Cell*, **19**, 1540–1547.
16. Berbari, N.F., Lewis, J.S., Bishop, G.A., Askwith, C.C. and Mykytyn, K. (2008) Bardet–Biedl syndrome proteins are required for the localization of G protein-coupled receptors to primary cilia. *Proc. Natl Acad. Sci. USA*, **105**, 4242–4246.
17. Davis, R.E., Swiderski, R.E., Rahmouni, K., Nishimura, D.Y., Mullins, R.F., Agassandian, K., Philp, A.R., Searby, C.C., Andrews, M.P., Thompson, S. *et al.* (2007) A knockin mouse model of the Bardet–Biedl syndrome 1 M390R mutation has cilia defects, ventriculomegaly, retinopathy, and obesity. *Proc. Natl Acad. Sci. USA*, **104**, 19422–19427.
18. Fath, M.A., Mullins, R.F., Searby, C., Nishimura, D.Y., Wei, J., Rahmouni, K., Davis, R.E., Tayeh, M.K., Andrews, M., Yang, B. *et al.* (2005) Mkks-null mice have a phenotype resembling Bardet–Biedl syndrome. *Hum. Mol. Genet.*, **14**, 1109–1118.
19. Mykytyn, K., Mullins, R.F., Andrews, M., Chiang, A.P., Swiderski, R.E., Yang, B., Braun, T., Casavant, T., Stone, E.M. and Sheffield, V.C. (2004) Bardet–Biedl syndrome type 4 (BBS4)-null mice implicate Bbs4 in flagella formation but not global cilia assembly. *Proc. Natl Acad. Sci. USA*, **101**, 8664–8669.
20. Nishimura, D.Y., Fath, M., Mullins, R.F., Searby, C., Andrews, M., Davis, R., Andorf, J.L., Mykytyn, K., Swiderski, R.E., Yang, B. *et al.* (2004) Bbs2-null mice have neurosensory deficits, a defect in social dominance, and retinopathy associated with mislocalization of rhodopsin. *Proc. Natl Acad. Sci. USA*, **101**, 16588–16593.
21. Bai, C.B., Stephen, D. and Joyner, A.L. (2004) All mouse ventral spinal cord patterning by hedgehog is Gli dependent and involves an activator function of Gli3. *Dev. Cell*, **6**, 103–115.
22. Corbit, K.C., Shyer, A.E., Dowdle, W.E., Gaulden, J., Singla, V., Chen, M.H., Chuang, P.T. and Reiter, J.F. (2008) Kif3a constrains beta-catenin-dependent Wnt signalling through dual ciliary and non-ciliary mechanisms. *Nat. Cell Biol.*, **10**, 70–76.
23. Haycraft, C.J., Banizs, B., Aydin-Son, Y., Zhang, Q., Michaud, E.J. and Yoder, B.K. (2005) Gli2 and Gli3 localize to cilia and require the intraflagellar transport protein polaris for processing and function. *PLoS Genet.*, **1**, e53.
24. Huangfu, D., Liu, A., Rakeman, A.S., Murcia, N.S., Niswander, L. and Anderson, K.V. (2003) Hedgehog signalling in the mouse requires intraflagellar transport proteins. *Nature*, **426**, 83–87.
25. Rohatgi, R., Milenkovic, L., Corcoran, R.B. and Scott, M.P. (2009) Hedgehog signal transduction by Smoothened: pharmacologic evidence for a 2-step activation process. *Proc. Natl Acad. Sci. USA*, **106**, 3196–3201.
26. Rohatgi, R., Milenkovic, L. and Scott, M.P. (2007) Patched1 regulates hedgehog signaling at the primary cilium. *Science*, **317**, 372–376.
27. Tran, P.V., Haycraft, C.J., Besschetnova, T.Y., Turbe-Doan, A., Stottmann, R.W., Herron, B.J., Chesebro, A.L., Qiu, H., Scherz, P.J., Shah, J.V. *et al.* (2008) THM1 negatively modulates mouse sonic hedgehog signal transduction and affects retrograde intraflagellar transport in cilia. *Nat. Genet.*, **40**, 403–410.
28. Gerdes, J.M., Liu, Y., Zaghloul, N.A., Leitch, C.C., Lawson, S.S., Kato, M., Beachy, P.A., Beales, P.L., DeMartino, G.N., Fisher, S. *et al.* (2007) Disruption of the basal body compromises proteasomal function and perturbs intracellular Wnt response. *Nat. Genet.*, **39**, 1350–1360.
29. Marion, V., Stoetzel, C., Schlicht, D., Messaddeq, N., Koch, M., Flori, E., Danse, J.M., Mandel, J.L. and Dollfus, H. (2009) Transient ciliogenesis involving Bardet–Biedl syndrome proteins is a fundamental characteristic of adipogenic differentiation. *Proc. Natl Acad. Sci. USA*, **106**, 1820–1825.
30. Ross, A.J., May-Simera, H., Eichers, E.R., Kai, M., Hill, J., Jagger, D.J., Leitch, C.C., Chapple, J.P., Munro, P.M., Fisher, S. *et al.* (2005) Disruption of Bardet–Biedl syndrome ciliary proteins perturbs planar cell polarity in vertebrates. *Nat. Genet.*, **37**, 1135–1140.
31. Wiens, C.J., Tong, Y., Esmail, M.A., Oh, E., Gerdes, J.M., Wang, J., Tempel, W., Rattner, J.B., Katsanis, N., Park, H.W. *et al.* (2010) Bardet–Biedl syndrome-associated small GTPase ARL6 (BBS3) functions at or near the ciliary gate and modulates Wnt signaling. *J. Biol. Chem.*, **285**, 16218–16230.
32. Villavicencio, E.H., Walterhouse, D.O. and Iannaccone, P.M. (2000) The sonic hedgehog-patched-gli pathway in human development and disease. *Am. J. Hum. Genet.*, **67**, 1047–1054.
33. Lechtreck, K.F., Johnson, E.C., Sakai, T., Cochran, D., Ballif, B.A., Rush, J., Pazour, G.J., Ikebe, M. and Witman, G.B. (2009) The *Chlamydomonas reinhardtii* BBSome is an IFT cargo required for export of specific signaling proteins from flagella. *J. Cell Biol.*, **187**, 1117–1132.
34. Yen, H.J., Tayeh, M.K., Mullins, R.F., Stone, E.M., Sheffield, V.C. and Slusarski, D.C. (2006) Bardet–Biedl syndrome genes are important in retrograde intracellular trafficking and Kupffer's vesicle cilia function. *Hum. Mol. Genet.*, **15**, 667–677.
35. Varjosalo, M., Li, S.P. and Taipale, J. (2006) Divergence of hedgehog signal transduction mechanism between *Drosophila* and mammals. *Dev. Cell*, **10**, 177–186.
36. Zhao, Y., Tong, C. and Jiang, J. (2007) Hedgehog regulates smoothened activity by inducing a conformational switch. *Nature*, **450**, 252–258.
37. Pazour, G.J., San Agustin, J.T., Follit, J.A., Rosenbaum, J.L. and Witman, G.B. (2002) Polycystin-2 localizes to kidney cilia and the ciliary level is elevated in orpk mice with polycystic kidney disease. *Curr. Biol.*, **12**, R378–R380.
38. Zhang, Q., Murcia, N.S., Chittenden, L.R., Richards, W.G., Michaud, E.J., Woychik, R.P. and Yoder, B.K. (2003) Loss of the Tg737 protein results in skeletal patterning defects. *Dev. Dyn.*, **227**, 78–90.
39. Cano, D.A., Murcia, N.S., Pazour, G.J. and Hebrok, M. (2004) Orpk mouse model of polycystic kidney disease reveals essential role of primary cilia in pancreatic tissue organization. *Development*, **131**, 3457–3467.
40. Moyer, J.H., Lee-Tischler, M.J., Kwon, H.Y., Schrick, J.J., Avner, E.D., Sweeney, W.E., Godfrey, V.L., Cacheiro, N.L., Wilkinson, J.E. and Woychik, R.P. (1994) Candidate gene associated with a mutation causing recessive polycystic kidney disease in mice. *Science*, **264**, 1329–1333.
41. Zhang, Q., Davenport, J.R., Croyle, M.J., Haycraft, C.J. and Yoder, B.K. (2005) Disruption of IFT results in both exocrine and endocrine abnormalities in the pancreas of Tg737(orpk) mutant mice. *Lab. Invest.*, **85**, 45–64.
42. Loktev, A.V., Zhang, Q., Beck, J.S., Searby, C.C., Scheetz, T.E., Bazan, J.F., Slusarski, D.C., Sheffield, V.C., Jackson, P.K. and Nachury, M.V. (2008) A BBSome subunit links ciliogenesis, microtubule stability, and acetylation. *Dev. Cell*, **15**, 854–865.
43. Corbit, K.C., Aanstad, P., Singla, V., Norman, A.R., Stainier, D.Y. and Reiter, J.F. (2005) Vertebrate Smoothened functions at the primary cilium. *Nature*, **437**, 1018–1021.
44. Qin, J., Lin, Y., Norman, R.X., Ko, H.W. and Eggenschwiler, J.T. (2011) Intraflagellar transport protein 122 antagonizes Sonic Hedgehog signaling and controls ciliary localization of pathway components. *Proc. Natl Acad. Sci. USA*, **108**, 1456–1461.
45. Huang, P. and Schier, A.F. (2009) Dampened hedgehog signaling but normal Wnt signaling in zebrafish without cilia. *Development*, **136**, 3089–3098.
46. Ocbina, P.J., Tuson, M. and Anderson, K.V. (2009) Primary cilia are not required for normal canonical Wnt signaling in the mouse embryo. *PLoS One*, **4**, 1–8.

47. Sugiyama, N., Tsukiyama, T., Yamaguchi, T.P. and Yokoyama, T. (2011) The canonical Wnt signaling pathway is not involved in renal cyst development in the kidneys of inv mutant mice. *Kidney Int.*, **79**, 957–965.
48. Lancaster, M.A., Gopal, D.J., Kim, J., Saleem, S.N., Silhavy, J.L., Louie, C.M., Thacker, B.E., Williams, Y., Zaki, M.S. and Gleeson, J.G. (2011) Defective Wnt-dependent cerebellar midline fusion in a mouse model of Joubert syndrome. *Nat. Med.*, **17**, 726–731.
49. Lancaster, M.A., Louie, C.M., Silhavy, J.L., Sintasath, L., Decambre, M., Nigam, S.K., Willert, K. and Gleeson, J.G. (2009) Impaired Wnt-beta-catenin signaling disrupts adult renal homeostasis and leads to cystic kidney ciliopathy. *Nat. Med.*, **15**, 1046–1054.
50. McDermott, K.M., Liu, B.Y., Tlsty, T.D. and Pazour, G.J. (2010) Primary cilia regulate branching morphogenesis during mammary gland development. *Curr. Biol.*, **20**, 731–737.
51. Simons, M., Gloy, J., Ganner, A., Bullerkotte, A., Bashkurov, M., Kronig, C., Schermer, B., Benzing, T., Cabello, O.A., Jenny, A. *et al.* (2005) Inversin, the gene product mutated in nephronophthisis type II, functions as a molecular switch between Wnt signaling pathways. *Nat. Genet.*, **37**, 537–543.
52. Ocbina, P.J., Eggenschwiler, J.T., Moskowitz, I. and Anderson, K.V. (2011) Complex interactions between genes controlling trafficking in primary cilia. *Nat. Genet.*, **43**, 547–553.
53. Blacque, O.E., Reardon, M.J., Li, C., McCarthy, J., Mahjoub, M.R., Ansley, S.J., Badano, J.L., Mah, A.K., Beales, P.L., Davidson, W.S. *et al.* (2004) Loss of *C. elegans* BBS-7 and BBS-8 protein function results in cilia defects and compromised intraflagellar transport. *Genes Dev.*, **18**, 1630–1642.
54. Chen, M.H., Wilson, C.W., Li, Y.J., Law, K.K., Lu, C.S., Gacayan, R., Zhang, X., Hui, C.C. and Chuang, P.T. (2009) Cilium-independent regulation of Gli protein function by Sufu in hedgehog signaling is evolutionarily conserved. *Genes Dev.*, **23**, 1910–1928.
55. Humke, E.W., Dorn, K.V., Milenkovic, L., Scott, M.P. and Rohatgi, R. (2010) The output of hedgehog signaling is controlled by the dynamic association between suppressor of fused and the Gli proteins. *Genes Dev.*, **24**, 670–682.
56. Tukachinsky, H., Lopez, L.V. and Salic, A. (2010) A mechanism for vertebrate hedgehog signaling: recruitment to cilia and dissociation of SuFu–Gli protein complexes. *J. Cell Biol.*, **191**, 415–428.
57. Lum, L., Zhang, C., Oh, S., Mann, R.K., von Kessler, D.P., Taipale, J., Weis-Garcia, F., Gong, R., Wang, B. and Beachy, P.A. (2003) Hedgehog signal transduction via smoothened association with a cytoplasmic complex scaffolded by the atypical kinesin, Costal-2. *Mol. Cell*, **12**, 1261–1274.